www.czasopisma.pan.pl PAN POLSKA AKADEMIA NAUK www.journals.pan.pl

Arch. Metall. Mater., Vol. 61 (2016), No 3, p. 1521–1528

DOI: 10.1515/amm-2016-0249

S.F. HASSAN*,#

Mg-ZrO_2 NANOCOMPOSITE: RELATIVE EFFECT OF REINFORCEMENT INCORPORATION TECHNIQUE

Abstract: In this study, ingot metallurgy and powder metallurgy processes were used to incorporate 0.2 and 0.7 vol% of nano-size ZrO_2 particles reinforcement to develop magnesium nanocomposite. Both of the processing methods led to reasonably fair reinforcement distribution, substantial grain refinement and minimum porosity in the nanocomposites. Strengthening effect of nano-ZrO_2 reinforcement in the magnesium matrix was greater when incorporated using the ingot metallurgy process. The matrix ductility and resistance to fracture were significantly improved due to the presence of nano-ZrO_2 reinforcement when incorporated using the powder metallurgy process. Tensile fracture surfaces revealed that the less-ductile cleavage fracture mechanism of hexagonal close packed magnesium matrix has changed to more ductile mode due to the presence of nano-ZrO2 particles in all the processed nanocomposites.

Keywords: Processing, Nanocomposite, Magnesium, Microstructure, Tensile properties

1. Introduction

Magnesium has a long history of application in industries including military, automobile, aerospace and biomedical [1-3]. Increasing demand for fuel efficiency, conservation of energy resources and environmental protection renewed the interest in magnesium due to lightweight (density is 1.738g-cm^{-3}) and availability. Hence, intensive research activities in the last few decades were mostly focused on the development of magnesium based new materials with improved strength and ductility. Discontinuous reinforcement was one of the major initiative successfully improved many of the properties of magnesium beyond the limits dictated by alloying process [4-10]. Type of reinforcement and its compatibility with the matrix during the processing are considered to be critical for the end properties of the reinforced materials. Reports suggests that extremely fine thermally stable oxide particle reinforcement, including zirconia (ZrO_2), was able to improve the mechanical properties of magnesium [7-10]. Polymorphic ZrO_2 particles has monoclinic crystal structure till 1170°C [11], which is expected to remain stable in magnesium [12] with good interfacial integrity [13] due to relatively low processing temperature. The very limited number of study on the nano-size ZrO_2 particle reinforced magnesium shows that ingot metallurgy (IM) and powder metallurgy (PM) were suitable processing routes. However, there was no reports in open literature suggesting any attempt ever made to study the relative effectiveness of these processing routes on the microstructure and mechanical properties of ZrO_2 particles reinforced magnesium. Accordingly, the primary aim of this study was to incorporate nano-size ZrO_2 particles into commercially pure magnesium using ingot metallurgy and powder metallurgy technique. Obtained nanocomposites were hot extruded and characterized for their microstructural characteristics and mechanical properties. Particular emphasis was placed to study the relative effectiveness of reinforcement incorporation method and the presence of nano-size ZrO_2 particle on the microstructure and mechanical properties of magnesium.

2. Materials and experimental procedures

In this study, matrix material was magnesium (HCP crystal structure with density of 1.74g/cm3 [1]) in turnings form with >99.9% purity in IM process and in particle form with ≥98.5% purity and size range of 60-300μm in PM process. Nano-size ZrO_2 (monoclinic crystal structure with density of 5.89g/cm^3 [11]) particles of 99.5% purity with an average size of 29-68-nm were used as reinforcement phase. Two different volume percentages i.e., 0.22 and 0.66 of reinforcement was used to develop the nanocomposites.

Ingot metallurgy processing technique for the nanocomposites involved melting and superheating the magnesium turnings with reinforcement particles to 750°C under inert Ar gas atmosphere in a graphite crucible. Electrical resistance heating was used. Superheated nanocomposite slurry was stirred at 460 rpm for 2.5 minutes using a ceramic coated twin blade (pitch 45°) steel stirrer to facilitate the incorporation and uniform distribution of the reinforcement particles in the metallic melt. The slurry was then released through an orifice at the base of the crucible, disintegrated by two jets of argon gas, and subsequently deposited in a metallic mold with 40-mm diameter. The synthesis of monolithic magnesium was carried out using similar steps except that no reinforcement particles were added. Deposited materials were machined to

* KING FAHD UNIVERSITY OF PETROLEUM & MINERALS, DHAHRAN, KINGDOM OF SAUDI ARABIA

Correspondence address: sfhassan@kfupm.edu.sa

35-mm diameter and sectioned in to pieces with 40-mm height.

Blend-press-sinter powder metallurgy technique involved mixing the magnesium matrix particles and reinforcement particles in a V-blender for 6-hours followed by cold compaction at a pressure of 97 bar (50-tons) to form billets of 35-mm diameter and 40-mm height. A uniaxial hydraulic press with 150-ton capacity was used. The compacted billets s were coated with colloidal graphite and sintered in tube furnace at 500°C for 2-hours under argon atmosphere. The synthesis of monolithic magnesium was carried out using similar steps without addition of reinforcement.

Primary processed reinforced and monolithic magnesium were hot extruded using an extrusion ratio of 19.14: 1 on a 150 ton hydraulic press. Extrusion was carried out at 250°C. Colloidal graphite was used as lubricant.

The density of the polished extruded ingot metallurgy and powder metallurgy processed nanocomposite and monolithic magnesium was measured using Archimedes' principle. Randomly selected from three samples were of each material and were weighed in air and in distilled water. An A&D ER-182A electronic balance with an accuracy of 0.0001g was used for weighing the samples. Theoretical density of each of the material was calculated, using rule-of-mixture principle to estimate porosity level in extruded condition.

Microstructural characteristics of ingot metallurgy and powder metallurgy processed nanocomposites and monolithic magnesium was studies on metallographically prepared samples. Reinforcement distribution, reinforcement-matrix interfacial integrity and grain morphology was studies using Hitachi S4100 Field-Emission Scanning Electron Microscope (FESEM) and OLYMPUS optical microscope. Scion image analysis system was used to determine the grain size

Macrohardness measurements were made on the polished extruded ingot metallurgy and powder metallurgy processed nanocomposites and monolithic magnesium samples in accordance with ASTM E18-08 standard. Rockwell 15T superficial scale was used.

Coefficient of thermal expansion (CTE) of ingot metallurgy and powder metallurgy processed nanocomposites and monolithic magnesium was determined using automated LINSEIS L75 Platinum series thermo-mechanical analyzer. Displacement of the specimens was measured as a function of temperature (in the range of 50-400 °C) using an alumina probe and was subsequently used to determine the coefficient of thermal expansion. The heating rate of the samples was maintained at 5°C/min. A sample length of 10 ± 2 mm was used in all of the tests.

Elongation-to-fracture tensile test were conducted on extruded samples of ingot metallurgy and powder metallurgy processed materials in accordance with ASTM test method

TABLE 1

Results of physical and microstructural characterization of developed materials

Materials	Primary process*	Density (g/cm^3)		Porosity (%)	Grains morphology	
		Theoretical	Experimental		size (µm)	Aspect ratio
Mg/0.0ZrO2	IM	1.7400	1.7397 ± 0.0009	0.02	49 ± 8	1.5 ± 0.4
	PM		1.7387 ± 0.0022	0.08	60 ± 10	1.6 ± 0.3
Mg/0.2 ZrO2	IM	1.7491	1.7466 ± 0.0024	0.15	8 ± 2 (84%↓)	1.6 ± 0.4
	PM		1.7436 ± 0.0010	0.32	13 ± 3 (78%↓)	1.6 ± 0.4
Mg/0.7 ZrO2	IM	1.7674	1.7644 ± 0.0037	0.17	5 ± 2 (90%↓)	1.6 ± 0.4
	PM		1.7599 ± 0.0007	0.42	13 ± 2 (78%↓)	1.5 ± 0.4

* IM = ingot metallurgy technique
PM = blend-press-sinter powder metallurgy technique

Table 2

Results of mechanical properties of nano-ZrO2 reinforced and monolithic magnesium

Materials	Primary process	CTE (µm/m-ºC)	Macrohardness (HR15T)	0.2% YS (MPa)	UTS (MPa)	Ductility (%)
Mg/0.0ZrO2	IM	28.4 ± 0.3	37 ± 1	97 ± 2	173 ± 1	7.4 ± 0.2
	PM	29.4 ± 0.3	43 ± 0	111 ± 5	189 ± 5	6.1 ± 2.3
Mg/0.2ZrO2	IM	27.9 ± 0.6 (1.8 %↓)	59 ± 1 (59%↑)	186 ± 2 (92%↑)	248 ± 4 (43%↑)	4.7 ± 0.2 (36%↓)
	PM	28.8 ± 0.8 (2.0 %↓)	56 ± 1 (30%↑)	140 ± 3 (26%↑)	160 ± 8 (15%↓)	6.4 ± 1.5 (5%↑)
Mg/0.7ZrO2	IM	26.4 ± 0.8 (7.0 %↓)	62 ± 1 (68%↑)	221 ± 5 (128%↑)	271 ± 6 (57%↑)	4.8 ± 0.7 (35%↓)
	PM	27.2 ± 0.9 (7.5 %↓)	58 ± 0 (35%↑)	163 ± 3 (47%↑)	202 ± 6 (7%↑)	11.4 ± 0.9 (87%↑)

E8M-09. Instron 8516 machine was used with a crosshead speed set at 0.254 mm/min on round tension test specimens of 5 mm diameter and 25 mm gauge length. Instron 2630-100 Series Clip-On type extensometer was used for strain recording. Fracture surfaces were studied using JEOL JSM-5600 LV scanning electron microscope to investigate the failure mechanisms.

3. Results

Macrostructural characterization of the ingot metallurgy processed deposited materials and powder metallurgy processed compacted billet did not reveal any macrostructural defects. Surfaces of the extruded nanocomposite and monolithic magnesium rods were smooth and free from any noticeable surface defects. Density measurement (see table 1) revealed that both the ingot metallurgy and powder metallurgy processes has effectively led to fabrication of near dense reinforced and monolithic magnesium in this study. However, level of porosity in the processed materials shows that ingot metallurgy process was more effective in producing near dense materials when compared to powder metallurgy process.

Microstructural characterization of the extruded samples showed that both ingot metallurgy and powder metallurgy processes used in this study were capable in dispersing nano-ZrO_2 particles in magnesium matrix with good reinforcement-matrix integrity (see Figure 1). Dispersed nano-ZrO_2 particles induced significant grain refinement in commercially pure magnesium (see Table 1). The result also shows that the ingot metallurgy process was relatively more effective than the powder metallurgy process in dispersing the increasing amount of nano-ZrO_2 particles and consequently exploiting their presence as grain refiner for the magnesium matrix.

Coefficient of thermal expansion characterization revealed that there was an increasing improvement in dimensional

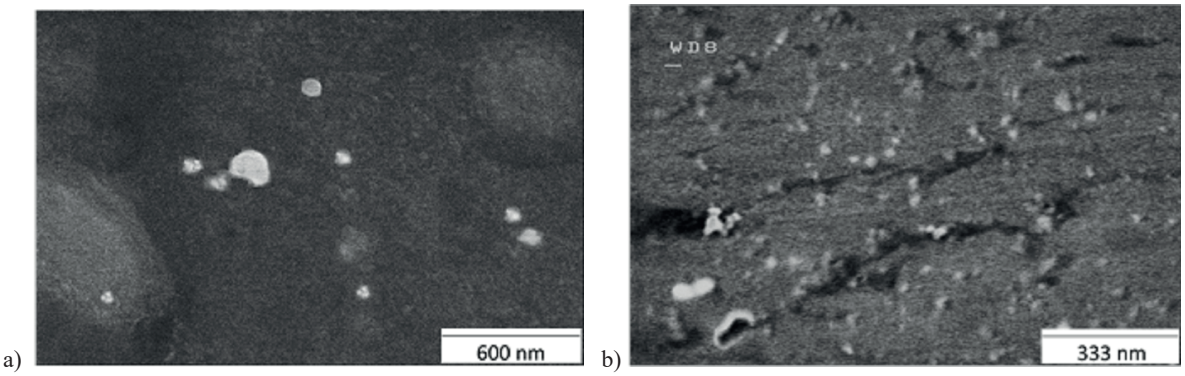

Fig. 1: Representative FESEM micrographs showing nano-ZrO2 distribution in the Mg/0.7ZrO2 nanocomposites processed using: (a) IM and (b) PM, respectively.

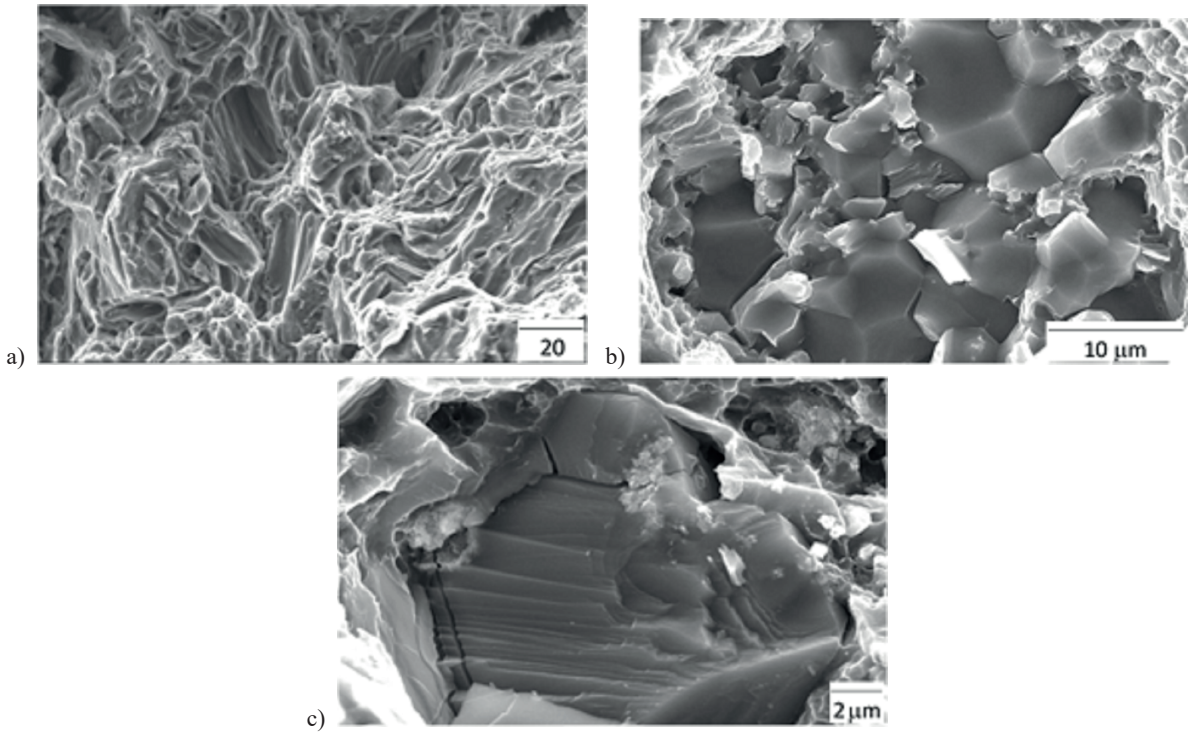

Fig. 2: Fractographs showing fracture features in ingot metallurgy processed materials: (a) cleavage in monolithic, and (b) intergranular crack propagation, and (c) microcracks in nano-ZrO2 particles incorporated magnesium matrix, respectively.

stability of ingot metallurgy and powder metallurgy processed magnesium matrix in the temperature range of 50-400°C (see Table 2) when reinforced with increasing volume percentage of nano-ZrO_2 particles.

Mechanical characterization revealed significant improvement in hardness and strength properties of magnesium (see Table 2) processed using ingot metallurgy and powder metallurgy process due to the increasing presence of nano-ZrO_2. Ductility of magnesium matrix was compromised in ingot metallurgy processed nanocomposite while enhanced in powder metallurgy processed nanocomposite. Dominating fracture mechanism in ZrO_2 particles reinforced magnesium matrix was intergranular crack propagation in ingot metallurgy processed nanocomposite (see Figure 2) and pseudo-dimple like feature indicating brittle-to-ductile transition in powder metallurgy processed nanocomposite (see Figure 3).

4. Discussion

Microstructural characteristics of the nano-ZrO_2 particles reinforced magnesium nanocomposites, processed using ingot and powder metallurgy process, are discussed in terms of: (a) reinforcement distribution pattern, (b) grain morphology, and (c) amount of porosity.

Reasonably uniform distribution of nano-ZrO_2 particles in magnesium matrices (see Figure 1) in both the ingot metallurgy and powder metallurgy processed materials can be attributed to the successive effect of primary and secondary processing parameters used in this study. In the case of ingot metallurgy processed nanocomposite, the reinforcement distribution pattern can be attributed to the cumulative effect of: (i) possible limited agglomeration of nano-ZrO_2 particles during melting of matrix due to homogeneous arrangement of raw matrix-reinforcement materials in crucible for melting and melt stirring, (ii) minimal gravity associated settlement due to the prudent selection of stirring parameters, (iii) reasonable good wetting of reinforcement particles by the matrix melt [13] and (iv) high extrusion ratio used in secondary processing. Almost zero standard deviation in the experimentally measured density values was also supportive to the uniform distribution of reinforcement in the ingot metallurgy processed materials. On other hand, the reinforcement distribution pattern in powder metallurgy processed materials can be attributed to the cumulative effect of: (i) suitable parameters for nano-ZrO_2 –magnesium particles blending, and (ii) high extrusion ratio used in secondary processing. Large deformation process assist in homogenous distribution of reinforcement particles in matrix regardless of the size difference between the matrix and reinforcement powder [14]. However, there was an increasing tendency of clustering of the nano-ZrO_2 particles [15] with their increasing volume percentage which was more evident in the case of powder metallurgy processed nanocomposites. Reinforcement-matrix interfacial integrity was assessed in terms of interfacial debonding and nanovoids and was found to be good as anticipated for metal-oxide system [13].

Metallography on the developed extruded materials revealed complete recrystallization of the matrices with significant refinement in near-equiaxed magnesium grains due to the presence of nano-ZrO_2 particles (see Table 1). Thermally stable nano-ZrO_2 particles acted as nucleation sites in recrystallization process during the secondary thermomechanical process and hence the increasing volume fraction of reinforcement particle induces enhanced grain refinement in the matrix. Relatively superior grain refinement in the ingot metallurgy processed reinforced nanocomposite could be attributed to the anticipated initial fine grained cast matrix, resulted from dispersed nano-ZrO_2 particles in matrix due to vigorous stirring of reinforcement-matrix slurry prior to the solidification. The dispersed enormous nano-ZrO_2 particles acted as nuclei in the solidifying melt and grain boundary pinning-site during progressive solidification [16]. Powder metallurgy primary processed reinforced magnesium also expected to experience grain refinement compared to the monolithic counterpart during sintering due to presence of enormous number of nano-ZrO_2 particles which acted as nuclei during recrystallization and grain boundary pinning-site during grain growth [16]. However, increasing tendency of reinforcement clustering limited the grain refinement effect of increasing volume percentage of nano- ZrO_2 particles in the powder metallurgy processed materials. In essence, ingot metallurgy process was relatively more effective in grain refinement of magnesium when reinforced with nano-ZrO_2 particles.

Minimal porosity in the processed reinforced nanocomposites, which also corroborated by the experimentally measured density values (see Table 1), could be attributed to the cumulative effect of parameters used in both primary and secondary process. However, ingot metallurgy process was relatively more effective in producing dense materials when compared to the powder metallurgy processed one.

Coefficient of thermal expansion characterization of the ingot metallurgy and powder metallurgy processed magnesium revealed increasing dimensional stability in the temperature range of 50-400°C (see Table 2), when incorporated with increasing volume percentage of nano-ZrO_2 particles reinforcement. This could be attributed to the synergic effect of: (i) lower CTE of the nano-ZrO_2 particle reinforcement (11.0 µm/m-ºC [17] for ZrO_2 and 27.045 µm/m-ºC [19] for Mg), (ii) relatively uniform distribution of the nano-ZrO_2 particles reinforcement in the matrix, and (iii) good reinforcement/matrix interfacial integrity. The results also revealed that both of the processing methods, ingot metallurgy and powder metallurgy, were almost equally effective in improving the dimensional stability of the commercially pure magnesium matrix by exploitation of the presence of nano-ZrO_2 particles with lower CTE.

Hardness measurements on the nano-ZrO_2 particles reinforced nanocomposite revealed that presence of the reinforcement led to significant increment in the superficial macrohardness of magnesium matrix (see Table 2) both in the ingot metallurgy processed condition (up to ~68%) and powder metallurgy processed condition (~35%). The hardness enhancement could primarily be attributed to the (i) presence of harder ceramic particles [5, 6], (ii) dispersed hard phase induced higher resistance to the localized deformation during test indentation, and (iii) reduced grain size. Relatively less-uniform distribution of nano-ZrO_2 particles and consequent lesser grain refinement caused limited hardness increment in powder metallurgy processed nanocomposite, which made

TABLE 3

Specific strength and work of fracture of nano-ZrO2 reinforced and monolithic magnesium

Materials	Primary process	Work of fracture (MJ/m³)[a]	$\sigma_{0.2\%YS}/\rho$ (kN-m/kg)	σ_{UTS}/ρ (kN-m/kg)
Mg/0.0ZrO2	IM	11.1 ± 0.3	56	99
	PM	9.7 ± 3.8	64	109
Mg/0.2ZrO2	IM	9.8 ± 0.9 (12%↓)	106 (89%↑)	142 (43%↑)
	PM	12.2 ± 2.8 (72%↑)	80 (5%↑)	92 (17%↓)
Mg/0.7ZrO2	IM	10.8 ± 1.5 (3%↓)	125 (123%↑)	154 (56%↑)
	PM	27.2 ± 1.9 (283%↑)	93 (22%↑)	115 (4%↑)

a Determined from engineering stress–strain diagram using EXCEL software

the ingot metallurgy process more effective in exploitation of hardening effect of nano-ZrO_2 particles in magnesium matrix.

Elongation-to-failure tensile test revealed increase in 0.2% yield strength and ultimate tensile strength of magnesium due to the incorporation of nano-ZrO_2 particles (see Table 2) by ingot metallurgy and powder metallurgy processes. The strengthening effect (including strain hardening) of nano-ZrO2 particles was significantly higher in ingot metallurgy processed nanocomposite compared to powder metallurgy processed nanocomposite.

Cumulative effect of various strengthening mechanisms apparently contributed to the enhancement in 0.2%yiled strength of magnesium due to the incorporation of nano-ZrO_2 particles:

(i) Orowan Strengthening Mechanism: increases yield strength of matrix due to the interaction between dislocation and dispersed fine hard reinforcement particle, especially if the particles are located within the grain. Orowan strengthening effect was anticipated to be significant in the ingot metallurgy processed reinforced nanocomposite (where nano-ZrO_2 particles located within grain and at the grain boundary) and insignificant in the powder metallurgy processed nanocomposite (where nano-ZrO_2 particles mostly located at the grain boundary).

(ii) Hall-Petch Strengthening Mechanism: increase yield strength of matrix due to the interaction between dislocation and increasing grain boundary according to the relation [19]

$\sigma^{HP} = \sigma_o + K/\sqrt{D}$, where σ_o the friction stress, D the grain size is and K is a constant depends on the stress direction. Hall-Petch strengthening effect was anticipated to be significantly higher in the cases of ingot metallurgy processed reinforced nanocomposites due to relatively superior grain refinement (see Table 1) compared to the nanocomposites processed using powder metallurgy process.

(iii) Increased Dislocation Density Strengthening: increases yield strength of matrix due to the increment in dislocation density, which generated due to the elastic modulus and coefficient of thermal expansion mismatch between nano-ZrO2 particles and magnesium matrix. Yield strength increment can follow the relation [20]:

$$\sigma_{my} = \sigma_{mo} + \Delta\sigma \tag{1}$$

Where σ_{my} and σ_{mo} are yield strength of the reinforced and unreinforced matrix material, respectively, and $\Delta\sigma$, the total increment in yield stress of the matrix due to the incorporation of nano-ZrO_2 particles can be estimated by [21]

$$\Delta\sigma = \sqrt{(\Delta\sigma_{EM})^2 + (\Delta\sigma_{CTE})^2} \tag{2}$$

Where $\Delta\sigma_{EM}$ and $\Delta\sigma_{CTE}$ are strength increment due to mismatch in elastic modulus (EM) and coefficient of thermal expansion (CTE) between reinforcement and matrix, and estimated as [21]:

$$\Delta\sigma_{EM} = \sqrt{3}\alpha\mu_m b\sqrt{\rho_G{}^{EM}} \tag{3}$$

$$\Delta\sigma_{CTE} = \sqrt{3}\beta\mu_m b\sqrt{\rho_G{}^{CTE}} \tag{4}$$

Where μ_m is matrix shear modulus, b is Burgers vector, and α and β are the two dislocation strengthening coefficients. The stiff and thermally stable reinforcement particles causes deformation incompatibility in matrix due to the presence of high dislocation density at their immediate adjacent location. Source of these geometrically necessary dislocations are differences in reinforcement-matrix elastic modulus (205 GPa [17, 19] for ZrO_2 and 45 GPa for Mg [18, 19]) and CTE (11.0 µm/m-ºC [17] for ZrO_2 and 27.045 µm/m-ºC [18] for Mg). Elastic modulus mismatch induced dislocation density can be estimated by [22]:

$$\rho_G{}^{EM} = \frac{4\gamma}{b\lambda} \tag{5}$$

Where γ is plastic shear strain, and λ is local length of the deformation field. For particle reinforced nanocomposites, λ is related to the interparticle distance and considered to be approximately equal to $r/(f)^{0.5}$, where r is the particle radius and f is the volume fraction of the particles.

CTE mismatch induced dislocation density can be estimated by [23]:

$$\rho_G^{CTE} = \frac{A\varepsilon V_p}{b(1-V_p)d} \quad (6)$$

Where A is a geometric constant, b is the Burgers vector, d is the diameter of the particle, V_p is the particle volume fraction and ε is the thermal misfit strain between the reinforcement and matrix. Equation justifies that the smaller diameter and higher volume fraction of the reinforcement will yield higher dislocation density in matrix.

Increases in $\Delta\sigma_{EM}$ and $\Delta\sigma_{CTE}$ with increasing volume of nano-ZrO_2 particles induced an increase in yield strength of reinforced nanocomposites samples (Eqs. (1)–(4) and Table 2).

Increased dislocation density strengthening mechanism was anticipated to be relatively significant in the ingot metallurgy processed reinforced nanocomposite due to relatively better reinforcement particle dispersion compared to the powder metallurgy processes reinforced nanocomposites.

There was an improvement of 0.2% yield strength and ultimate tensile strength of the magnesium matrix for all the nanocomposites in this current investigation except for the powder metallurgy processed 0.2 volume percentage reinforcement contained one, where insufficient strain hardening reduced the ultimate tensile strength of the matrix.

Ductility of the nano-ZrO_2 particles reinforced magnesium matrices (see Table 2) was adversely affected when incorporated using ingot metallurgy but significantly improved in the presence of increasing presence of reinforcement incorporated using powder metallurgy process. Presence of extremely fine oxides [9, 10] reportedly improved the room temperature ductility of the less ductile magnesium when uniformly dispersed [24] and refined grains [25]. However, despite relatively better reinforcement particle dispersion and higher grain refinement induced intergranular crack propagation (see Figure 2b) and presence of large number of microcrack (see Figure 2c) led to the resultant reduced ductility in the ingot metallurgy processed nano-ZrO_2 particles reinforced magnesium nanocomposite. However, pseudo-dimples (see Figure 3b) due to easy multidirectional dislocation motion (see Figure 3c) [26] and intergranular crack propagation (see Figure 3d) led to improved ductility in powder metallurgy processed matrices of developed nanocomposites.

The energy absorption capacity were calculated in terms of work of fracture using the stress-strain graphs [19], which revealed (see Table 3) that powder metallurgy processed nano-ZrO_2 particles reinforced nanocomposites were distinctly superior in fracture resistance compared to those processed using ingot metallurgy technique.

The result of this study revealed that ingot metallurgy process was effective in improving the strength characteristic and powder metallurgy process was effective in improving the ductility and work of fracture of the magnesium matrices due to the increasing incorporation of the nano-ZrO_2 particles as reinforcement. Ingot metallurgy processing of the nano-ZrO_2 particles reinforced nanocomposites were effective for strength based designs (higher yield strength when compared to monolithic magnesium) while the powder metallurgy processing of the nano-ZrO_2 particles reinforced nanocomposites were effective for damage tolerant designs (higher work of fracture when compared to monolithic magnesium).

Tensile fractured surfaces of the processed materials revealed microstructural effect on the tensile properties of the nano-ZrO2 particles reinforced magnesium matrices. Presence of microscopically rough small steps, both in ingot metallurgy

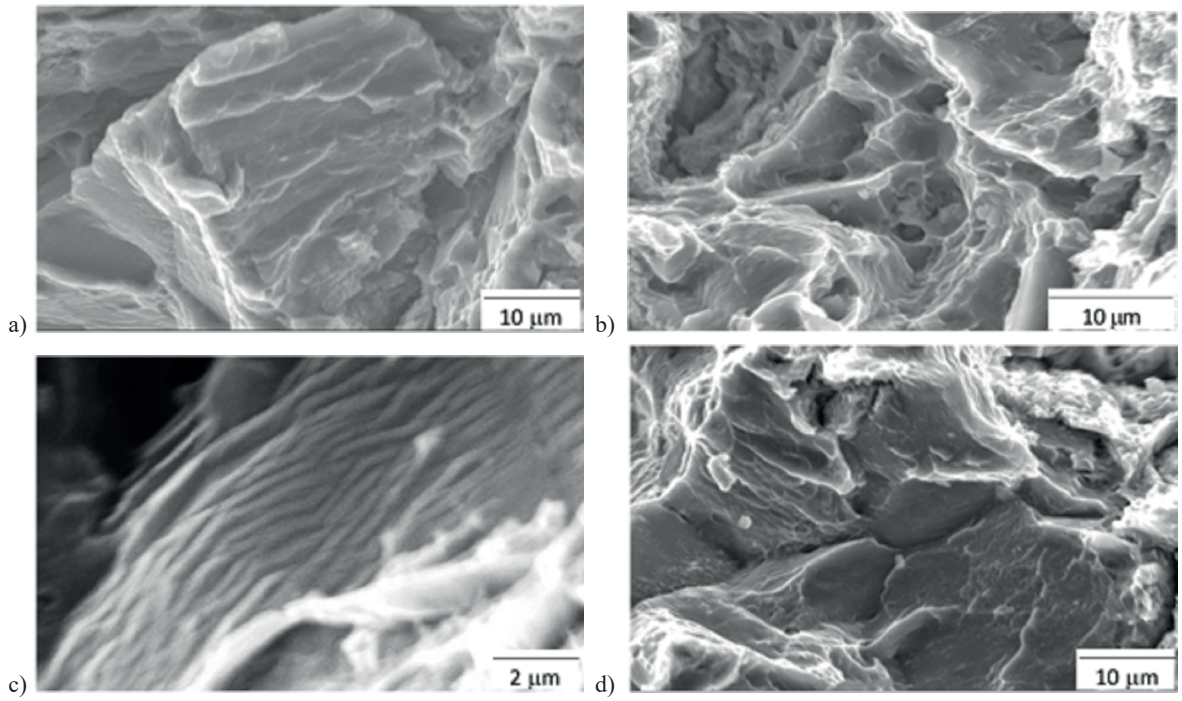

Fig. 3: Fractographs showing fracture features in powder metallurgy processed materials: (a) cleavage in monolithic, and (b) pseudo-dimple, (c) uneven dislocation motion indicating easy multidirectional dislocation motion, and (d) intergranular crack propagation in nano -ZrO_2 particles incorporated magnesium matrices, respectively

processed (see Figure 2a) and powder metallurgy processed (see Figure 3a) monolithic magnesium, indicating its relatively less ductile nature [27]. Incorporation of nano-ZrO_2 particles led the fracture mechanism of magnesium to be more ductile in nature, dominating intergranular crack propagation (see Figure 2b) in the ingot metallurgy processed magnesium matrices. However, presence of large number of microcrack (see Figure 2c) compromised the benefit of intergranular cracking in the hexagonal close pack structured [25] magnesium. On the other hand, the pseudo-dimples (see Figure 3b), indicating ductile failure [19], were dominating fracture mode in powder metallurgy processed nano-ZrO_2 particles reinforced magnesium matrices. Intergranular crack propagation (see Figure 3d) acted as less dominating failure mode in the powder metallurgy processed reinforced nanocomposite.

5. Conclusions

Traditional ingot metallurgy and blend-press-sinter powder metallurgy processes were competent to synthesize nano-ZrO_2 particles reinforced light weight magnesium nanocomposite with effective reinforcement distribution.

Ingot metallurgy process was relatively more effective in dispersion of nano-ZrO_2 particles and consequently grains refinement and strengthening of magnesium matrix when compared to the powder metallurgy process.

Ingot metallurgy and powder metallurgy processes were equally effective in improving dimensional stability of magnesium matrix by the presence of nano-ZrO_2 particles.

Powder metallurgy process was relatively more effective in improving the formability and resistance to fracture of magnesium matrices by nano-ZrO_2 particles reinforcement when compared to the ingot metallurgy process.

Acknowledgement:

The authors would like to acknowledge the support provided by King Fahd University of Petroleum and Minerals (KFUPM) for this research effort.

REFERENCES

[1] K.U. Kainer, F. Von Buch, Magnesium – Alloys and Technology, (K.U. Kainer Edited)), WILEY-VCH Verlag GmbH & Co. KGaA, Weinheim (2003).
[2] I. Ostrovsky, Y. Henn, In: International Conference "New Challenges in Aeronautics" ASTEC'07, Moscow (2007).
[3] F. Witte, Acta Biomater. **6**, 1680–1692 (2010).
[4] D.J. Lloyd, Int. Mater. Rev. **39**, 1 -23 (1994).
[5] R. Unverricht, V. Peitz, W. Riehemann, H. Ferkel, In: Conference on Magnesium Alloys and Their Applications, Germany (1998).
[6] H. Ferkel, B.L. Mordike, Mat. Sci. Eng. A-Struct. **298**, 193-199 (2001).
[7] S.F. Hassan, M.J. Tan, M. Gupta, Mater. Sci. Tech. **23**, 1309-1312 (2007).
[8] S.F. Hassan, M. Gupta, J. Compos. Mater. **41**, 2533-2543 (2007).
[9] S.F. Hassan, M. Gupta, Compos. Struct. **72**, 19-26 (2006).
[10] S.F. Hassan, Mat. Sci. Eng. A-Struct. **528**, 5484–5490 (2011).
[11] R. Morrell, Handbook of Properties of Technical and Engineering Ceramics, Part 1: An Introduction for the Engineer and Designer, Her Majesty's Stationary Office, England, UK, (1985).
[12] J.D. Gilchrist, Extraction Metallurgy, 3rd edn., Pergamon Press, Great Britain, (1989).
[13] N. Eustathopoulos, M.G. Nicholas, B. Drevet, Wettability at High Temperatures. Pregamon Materials Series, Elsevier, UK, (1999).
[14] M.J. Tan, X. Zhang, Mat. Sci. Eng. A-Struct. **244**, 80–85 (1998).
[15] G.N. Hassold, E.A. Holm, D.J. Srolovitz, Scripta Metall. Mater. **24**, 101-106 (1990).
[16] Y.C. Lee, A.K.| Dahle, D.H. StJohn, Metall. Mater. Trans. A 31, 2895-2906 (2000).
[17] Website: <https://www.ceramicindustry.com/ext/resources/pdfs/2013-CCD-Material-Charts.pdf> last assessed May 2015.
[18] C.J. Smithells, Metals Reference Book, 7th edn, Butterworth-Heinemann Ltd, London, (1992).
[19] W.D. Callister, Materials Science and Engineering: An Introduction, John-Wiley & Sons, Inc., New York, USA (2007).
[20] L.H. Dai, Z. Ling, Y.L. Bai, Compos. Sci. Technol.**61**, 1057–1063 (2001).
[21] T.W. Clyne, P.J. Withers. An Introduction to Metal Matrix Composites. Cambridge University Press New York, USA, (1993).
[22] N.A. Fleck, G.M. Muller, M.F. Ashby, J.W. Hutchinson, Acta Metall. Mater. **42**, 475–487 (1994).
[23] N. Chawla, K.K. Chawla, Metal Matrix Composites. New York: Springer Science + Business Media, Inc.(2006).
[24] G.S. Ansell, Physical metallurgy, (ed. R.W. Cahn), North-Holland Publishing Company, Amsterdam (1970).
[25] W. Yang, W.B. Lee, Mesoplasticity and its applications, Springer-Verlag, Berlin (1993).
[26] P. Pérez, G. Garcés, P. Adeva, Compos. Sci. Technol.**64**, 145-151 (2004).
[27] G.V. Raynor, The Physical Metallurgy of Magnesium and Its Alloys, Pergamon Press Ltd., Britain (1959).